Development 134, 2771-2781 (2007) doi:10.1242/dev.004531

Zebrafish *relatively relaxed* mutants have a ryanodine receptor defect, show slow swimming and provide a model of multi-minicore disease

Hiromi Hirata[1,2,†], Takaki Watanabe[1], Jun Hatakeyama[3], Shawn M. Sprague[2], Louis Saint-Amant[2,*], Ayako Nagashima[2], Wilson W. Cui[2], Weibin Zhou[2] and John Y. Kuwada[2]

Wild-type zebrafish embryos swim away in response to tactile stimulation. By contrast, *relatively relaxed* mutants swim slowly due to weak contractions of trunk muscles. Electrophysiological recordings from muscle showed that output from the CNS was normal in mutants, suggesting a defect in the muscle. Calcium imaging revealed that Ca^{2+} transients were reduced in mutant fast muscle. Immunostaining demonstrated that ryanodine and dihydropyridine receptors, which are responsible for Ca^{2+} release following membrane depolarization, were severely reduced at transverse-tubule/sarcoplasmic reticulum junctions in mutant fast muscle. Thus, slow swimming is caused by weak muscle contractions due to impaired excitation-contraction coupling. Indeed, most of the ryanodine receptor 1b (*ryr1b*) mRNA in mutants carried a nonsense mutation that was generated by aberrant splicing due to a DNA insertion in an intron of the *ryr1b* gene, leading to a hypomorphic condition in *relatively relaxed* mutants. RYR1 mutations in humans lead to a congenital myopathy, multi-minicore disease (MmD), which is defined by amorphous cores in muscle. Electron micrographs showed minicore structures in mutant fast muscles. Furthermore, following the introduction of antisense morpholino oligonucleotides that restored the normal splicing of *ryr1b*, swimming was recovered in mutants. These findings suggest that zebrafish *relatively relaxed* mutants may be useful for understanding the development and physiology of MmD.

KEY WORDS: Zebrafish, Ryanodine receptor, Muscle, Calcium, Multi-minicore disease

INTRODUCTION

Zebrafish are useful for the study of motor development and disorders. First, forward genetics can be applied to this organism to identify genes that are essential for proper behaviors (Granato et al., 1996). Second, embryos are transparent, facilitating the visualization of dynamic events, such as cell migration, axonal outgrowth and calcium transients, in live fish (Fetcho and Bhatt, 2004; Wilson et al., 2002). Third, electrophysiological techniques can be used to analyze the physiology of embryonic neurons and muscles (Drapeau et al., 2002; Fetcho, 2006). Fourth, zebrafish embryos exhibit readily assayable and well-characterized behaviors (Eaton and Farley, 1973; Saint-Amant and Drapeau, 1998). Fifth, zebrafish mutants can potentially serve as animal models of human motor disorders (Bassett and Currie, 2003; Kunkel et al., 2006; Lieschke and Currie, 2007).

Zebrafish embryos display three stereotyped behaviors by 36 hours post-fertilization (hpf) (Saint-Amant and Drapeau, 1998). The earliest behavior consists of repetitive, slow and alternating coiling of the trunk and tail. This coiling is independent of sensory stimulation and observed from 17 to 26 hpf. After 21 hpf, embryos respond to mechanosensory stimulation with two or three rapid C-bends of the trunk and tail. By 26 hpf, embryos swim in response to tactile stimulation. The frequency of muscle contractions during swimming increases from 7 Hz at 26 hpf to 30 Hz at 36 hpf, the latter being similar to the frequency of swimming by adult zebrafish (Buss and Drapeau, 2001).

The process of touch-induced swimming involves a number of steps, starting with the sensing of tactile stimuli and ending with the contraction of muscles. Touch is sensed by Rohon-Beard neurons in the trunk and tail or trigeminal sensory neurons in the head (Drapeau et al., 2002). Once triggered by sensory inputs, interneuronal networks located in the hindbrain and spinal cord create the appropriate motor pattern that alternately activates motor neurons in each side of the spinal cord (Fetcho, 1992; Gahtan et al., 2002). Motor terminals release acetylcholine at the neuromuscular junction (NMJ) to depolarize the muscle membrane (Buss and Drapeau, 2001; Wen and Brehm, 2005) and the change of membrane potential is converted to muscle movement by excitation-contraction (E-C) coupling (Franzini-Armstrong and Protasi, 1997). Depolarizations of the plasma membrane spread down the transverse-tubules (t-tubules), which are invaginations of the plasma membrane, and cause conformational changes of the dihydropyridine receptor (DHPR), a voltage sensor located in the t-tubule membrane. DHPRs then trigger the opening of ryanodine receptor 1 (RyR1) in the adjacent sarcoplasmic reticulum (SR) to allow Ca^{2+} release from the SR to the cytosol (Meissner, 1994). Elevated cytoplasmic Ca^{2+}, in turn, activates the sliding of actin/myosin to produce muscle contraction.

The membranes of t-tubules and SR are juxtaposed and permit direct physical interactions between DHPR and RyR1 in skeletal muscle (Block et al., 1988). The skeletal muscle DHPR is composed of the voltage-sensing and pore-forming α1S subunit, intracellular modulatory β1 subunit, and auxiliary $\alpha2\delta1$ and γ1 subunits (Catterall, 2000; Flucher et al., 2005). A tetrad, which is a cluster of four DHPRs, associates with a Ca^{2+}-releasing RyR1 channel, which is formed with four RyR1 monomers. The RyR1 protein, the largest known ion channel protein, weighs 560 kDa

[1]Graduate School of Science, Nagoya University, Nagoya 464-8602, Japan. [2]Department of Molecular, Cellular and Developmental Biology, University of Michigan, Ann Arbor, MI 48109-1048, USA. [3]Institute of Molecular Embryology and Genetics, Kumamoto University, Kumamoto 860-0811, Japan.

*Present address: Département de Pathologie et Biologie Cellulaire, Université de Montréal, Montréal, Québec, H3T 1J4, Canada
†Author for correspondence (e-mail: hhirata@bio.nagoya-u.ac.jp)

Accepted 29 May 2007

(Takeshima et al., 1989) and, thus, RyR1 channels can be observed in electron micrographs as dots of high electronic density (Franzini-Armstrong and Protasi, 1997). Although a hydrophobic C-terminus domain might contain several transmembrane domains as well as the channel pore, the exact number and position of membrane domains is not known. Three RyR isoforms (RyR1, RyR2 and RyR3) are encoded by different genes in mammals (Fill and Copello, 2002). RyR1 is the most abundant isoform in skeletal muscle. RyR2 predominantly functions in cardiac muscle and RyR3 is expressed by many tissues, but at relatively low levels. RyR1-deficient mice do not move because of the absence of E-C coupling and die from dysfunction of the diaphragm muscles shortly after birth (Takeshima et al., 1994). The formation of DHPR tetrads is also impaired in RyR1-deficient myotubes (Takekura et al., 1995).

Mutations in RyR1, encoded by the RYR1 gene in humans, are involved in a pharmacogenetic muscle disorder, malignant hyperthermia (MH), and two congenital myopathies, central-core disease (CCD) and multi-minicore disease (MmD). Inherited as a dominant trait, MH appears as a hypermetabolic crisis when a susceptible individual is exposed to certain anesthetics, such as halothane (MacLennan and Phillips, 1992). CCD is caused by a dominant RYR1 mutation, with two recessive exceptions, and is characterized by infantile hypotonia and muscle weakness (Zhang et al., 1993). Amorphous central cores, which run along the long axis of the muscle fibers, can be observed in histological sections of CCD muscle. MmD is characterized by muscle weakness, scoliosis and respiratory insufficiency, but is inherited through a recessive RYR1 mutation (Engel, 1967; Jungbluth et al., 2004). MmD is defined by the presence of multiple small cores in histological sections. Although little is known about the development of cores, it has been proposed that cores are formed as a secondary cellular response to isolate regions of defective Ca^{2+} regulation from regions of normal Ca^{2+} homeostasis (Lyfenko et al., 2004).

In this paper, we characterized the *relatively relaxed* (*ryr*) mutant, which was identified as a spontaneous mutation in our breeding stock of zebrafish. Mutants displayed slow swimming due to weak muscle contractions despite normal output from the CNS. Ca^{2+} transients in the muscle cytosol and RyR1 at the t-tubules were dramatically decreased in mutant fast muscles, suggesting a defect in E-C coupling. In fact, most of the *ryr1b* mRNA, encoding RyR1, carried a nonsense mutation in *relatively relaxed* mutants. Analysis of genomic DNA found an insertion in an intron of the *ryr1b* gene that resulted in aberrant splicing and a premature stop codon. Similar to human MmD, *relatively relaxed* mutants displayed small amorphous cores in muscle fibers. Interestingly, application of antisense morpholino oligonucleotides against *ryr1b* that blocked the aberrant splicing in mutants restored normal swimming. These findings suggest that analysis of the *relatively relaxed* mutant may be useful for understanding the development of amorphous cores and the physiology of MmD.

MATERIALS AND METHODS

Animals

Zebrafish were bred and raised according to established procedures (Nüsslein-Volhard and Dahm, 2002; Westerfield, 2000), which meet the guidelines set forth by the University of Michigan and Nagoya University. *ryr*^{mi340} was identified as a spontaneous mutation in our breeding stock of zebrafish.

Video-recording of zebrafish behavior

Embryonic behaviors were observed and video-recorded using dissection microscopy. Mechanosensory stimuli were delivered to the tail with forceps. Videos were captured with a CCD camera (WVBP330, Panasonic) and a frame grabber (LG-3, Scion Corporation), and were analyzed with Scion Image on a G4 Macintosh (Apple).

Muscle recording

The dissection protocols for in vivo patch recordings have been described elsewhere (Buss and Drapeau, 2000). Briefly, 48 hpf zebrafish embryos were anaesthetized in 0.02% tricaine (ethyl 3-aminobenzoate methanesulfonate, Sigma), pinned on a Sylgard dish and immersed in Evans solution (134 mM NaCl, 2.9 mM KCl, 2.1 mM $CaCl_2$, 1.2 mM $MgCl_2$, 10 mM glucose and 10 mM Hepes at 290 mOsm and pH 7.8). The skin was peeled off to allow access to the underlying muscles. For electrophysiological recordings, embryos were partially curarized in Evans solution containing 3 μM d-tubocurarine (Sigma) without tricaine. Patch electrodes were pulled from borosilicate glass (Narishige) to yield electrodes with resistances of 3-10 MΩ. The electrode was visually guided to patch muscle cells using Hoffman modulation optics (40× water immersion objective). The electrode solution consisted of 105 mM potassium gluconate, 16 mM KCl, 2 mM $MgCl_2$, 10 mM Hepes, 10 mM EGTA and 4 mM Na_3ATP at 273 mOsm and pH 7.2. Recordings were performed with an Axopatch 200B amplifier (Axon Instruments), low-pass filtered at 5 kHz and sampled at 10 kHz. Data were collected with Clampex 8.2 and analyzed with Clampfit 9.0 (both Axon Instruments). Mechanosensory stimulation was delivered by ejecting bath solution (20 psi, 20 milliseconds pulse) from a pipette with a 20 μm tip to the tail of the pinned embryo using a Picospritzer III (Parker Hannifin Corporation) to induce fictive swimming.

Ca^{2+} imaging in muscle

The protocols for Ca^{2+} imaging have been described previously (Hirata et al., 2004). Briefly, we injected Calcium Green-1 dextran (10,000 M_r, Molecular Probes) into one blastomere of 8- to 16-cell-stage progeny of *ryr* carrier in-crosses. At 48 hpf, embryos were anaesthetized with 0.02% tricaine and pinned to a Sylgard dish with tungsten wires. The tricaine was washed out and embryos were bathed in Evans solution with 5 mM of the muscle myosin inhibitor, N-benzyl-p-toluene sulphonamide (Sigma) (Cheung et al., 2002) to immobilize embryos. Mechanosensory stimulation was applied by ejecting bath solution using a Picospritzer III to the tail of the pinned embryos. Line-scanning of a Calcium Green-1 dextran-labeled muscle cell at 800 Hz was performed by confocal microscopy (FV-500, Olympus). After imaging, the genotype of the embryos was determined by genomic PCR.

Pharmacological treatment

Ruthenium red (Sigma), an inhibitor of RyR1 (Pessah et al., 1985), was diluted to 0.5 mg/ml in Evans solution and applied to embryos 1 hour before behavioral assay.

Mapping

ryr carrier fish were crossed with wild-type WIK fish to generate mapping carriers that were crossed to identify mutants for meiotic mapping to microsatellites (Gates et al., 1999; Shimoda et al., 1999), as described previously (Bahary et al., 2004). The LN54 radiation hybrid panel was used for the physical mapping (Hukriede et al., 1999).

Cloning of *ryr1b* cDNA

Twelve overlapping cDNA fragments covering the coding region of *ryr1b* were cloned by reverse transcriptase (RT)-PCR with the following primers: forward primer 1, 5′-GAGAAAACGCACGGATTTTCTGATTTCTCC-3′; reverse primer 1, 5′-CTGTGTAAAAAGGCCTGTGGTGCTGTAGAT-3′; forward primer 2, 5′-CTGCTCTCGCTCTCAGACAGAAGAGTC-3′; reverse primer 2, 5′-AGCAGTGTCAACAGGACAGGGAGTGAATG-3′; forward primer 3, 5′-CCTCCTCCTGGTTATGCACCATGTTATGAG-3′; reverse primer 3, 5′-TCAATGTGGTTGTGATCAGTGGGAACGGGA-3′; forward primer 4, 5′-CATCTGTGGCCTCCAAGAGGGCTTTG-3′; reverse primer 4, 5′-ACACACGGCGCAATAAAGCATCAGAGTGTG-3′; forward primer 5, 5′-TCCTGGAACTATCTGAGCAACATGACCTGC-3′; reverse primer 5, 5′-AAGACTGAACATGAGTCGCACCAGCTCTG-3′; forward

primer 6, 5′-GTTGATATCCCACACAATGATCCACTGGGC-3′; reverse primer 6, 5′-AACAGTGGGGCACATTTAGTGAGCAGAGG-3′; forward primer 7, 5′-CACCACAGAAATGGCTCTGGCTCTGAAC-3′; reverse primer 7, 5′-CTTAAAGTACTGGTTTATGAGCGGGAGCAG-3′; forward primer 8, 5′-GGAAGAGTTGAAAAATCCCCACACGAACAG-3′; reverse primer 8, 5′-ATCACCACAAAGTTCTGCTCCTCTCGCTTG-3′; forward primer 9, 5′-GAAGTCTTCATCTTCTGGTCTAAATCGCAC-3′; reverse primer 9, 5′-TGCAGTCTGAGCAGAAAGTCTACTGTGCAG-3′; forward primer 10, 5′-AACTACCGGCGCACACAAACAGGCAG-3′; reverse primer 10, 5′-ACGTCATCTTTTTAGCTCCCTCCACGAGAC-3′; forward primer 11, 5′-CTTGCTGATCTGGAACACTCTCTTTGGAG-3′; reverse primer 11, 5′-GTGTATTAAGGACTAGTCGGTCCCATTGG-3′; forward primer 12, 5′-CTGGCCCGTAAACTGGAGTTTGATGGTC-3′; reverse primer 12, 5′-AGGAGAGTTAAGTCAAGGCTACAGTCGGTC-3′.

PCR

The following primers were used for RT-PCR and genomic PCR: Primer #1, 5′-GTGGGTTTCTTGCCCGATATGAGAGCTTCA-3′; Primer #2, 5′-AACAGTGGGGCACATTTAGTGAGCAGAGG-3′.

Knockdown by morpholino

To knockdown RyR1b protein synthesis (Nasevicius and Ekker, 2000), antisense morpholino (MO)1 was designed against splice donor site of exon48: *ryr1b* MO1, 5′-ATGATTGAGTTTACCGTATCCAGAG-3′.

Standard control MO (randomized sequence available from Gene Tools) was used for control MO: control MO, 5′-CCTCTTACCTCAGTTACA-ATTTATA-3′.

For inhibition of aberrant splicing of *ryr1b* mRNA, antisense MO2 and MO3 were respectively designed against acceptor and donor sites of the aberrant exon: *ryr1b* MO2, 5′-ATTGGTTGACTCCTGATACTCAATG-3′; *ryr1b* MO3, 5′-TATCTTACACTTACCTTTAAATAAG-3′.

Injections were performed as described previously (Nüsslein-Volhard and Dahm, 2002).

Immunostaining

Zebrafish embryos were anaesthetized in 0.02% tricaine and pinned on a Sylgard dish with tungsten wires. After peeling off the skin at trunk region, embryos were fixed in 4% paraformaldehyde at room temperature for 20 minutes and then subjected to immunostaining as described previously (Hirata et al., 2005). The following primary antibodies were used: anti-RyR: 34C, IgG1 isotype, Sigma, 1/1000 (Airey et al., 1990); anti-DHPRα1: 1A, IgG1 isotype, Affinity BioReagents, 1/200 (Morton and Froehner, 1987); anti-DHPRβ: $VD2_1B12$, IgG1 isotype, Developmental Studies Hybridoma Bank, 1/2 (Leung et al., 1988); anti-DHPRα2: 20A, IgG2a isotype, Affinity BioReagents, 1/200 (Morton and Froehner, 1989). Alexa Fluor 488-conjugated anti-mouse IgG, Alexa Fluor 488-conjugated anti-mouse IgG1 and Alexa Fluor 555-conjugated anti-mouse IgG2a were used as secondary antibodies (1/1000, Molecular Probes).

In situ hybridization

In situ hybridizations to wholemounted zebrafish were performed as described previously (Hirata et al., 2004). For sectioning after color development, embryos were equilibrated in 15% sucrose/7.5% gelatin in PBS at 37°C and then embedded in it at –80°C. Sections (10 μm) were cut with a cryostat (CM3050S, Leica). An *ryr1b* probe covering 1089 bp of the C-terminus amino acids and 148 bp of the 3′-UTR was used for in situ hybridization. An *ryr1a* probe covering 1157 bp of the C-terminus was cloned with the following primers: *ryr1a* forward primer, 5′-ATGGTGAGAAGGCTGAGAAGGAAGTGGAGG-3′; *ryr1a* reverse primer, 5′-CGTCATCATGTCGTCACACTTCATGTCCGG-3′.

Transmission electron microscopy

The protocols for transmission electron microscopy have been described elsewhere (Hatakeyama et al., 2004; Schredelseker et al., 2005). Briefly, embryos were fixed with 6% glutaraldehyde-2% paraformaldehyde in 0.1 M sodium cacodylate buffer, pH 7.2, overnight at 4°C. After being washed in 0.1 M sodium cacodylate buffer, the embryos were post-fixed with 1% OsO_4 for 60 minutes, and then dehydrated and embedded in Epon 812. Ultrathin sections (80 nm) were cut and examined using an electron microscope (H-7000, Hitachi) operated at 75 kV.

RESULTS

ryr mutants show slow swimming because of weak muscle contractions

An autosomal, recessive mutation, *relatively relaxed* (ryr^{mi340}), was identified from our breeding stock of zebrafish. Mutant embryos exhibited significantly slower swimming after 36 hpf, but spontaneous coiling at 22 hpf (wild-type siblings: 0.21±0.11 Hz, n=34; *ryr* mutants: 0.19±0.09 Hz, n=14) and touch-induced fast C-bends at 24 hpf were unperturbed (data not shown). The swimming phenotype was examined by video-microscopy, with wild-type embryos swimming away rapidly upon tactile stimulation and *ryr* embryos swimming away much less efficiently (wild-type at 36 hpf: 1.61±0.44 cm/s, n=12; *ryr* at 36 hpf: 0.71±0.16 cm/s, n=12; Student's t-test, P<0.001; Fig. 1A-O, and see Movies 1,2 in the supplementary material). To examine the frequency and strength of contractions during swimming, 48 hpf embryos were video-recorded with their heads restrained on a Sylgard dish, leaving the

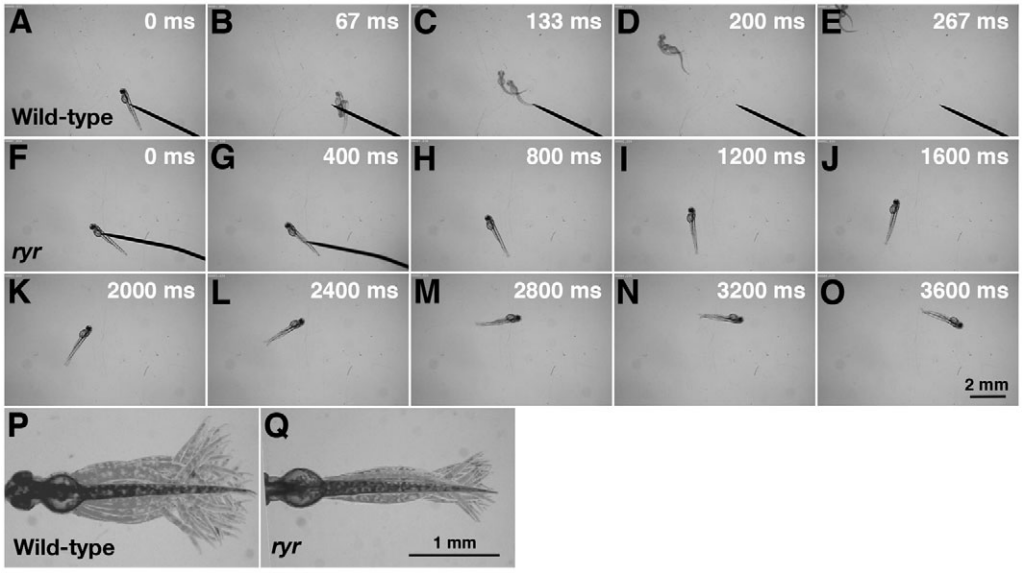

Fig. 1. *ryr* mutant embryos exhibit slow swimming and weak muscle contractions in response to touch. (**A-E**) Mechanosensory stimulation induced a wild-type embryo (48 hpf) to swim away rapidly. (**F-O**) Touch induced an *ryr* mutant embryo (48 hpf) to swim, but only slowly. (**P**) Superimposition of all the frames from a video showing normal displacement of the trunk and tail during a swimming episode induced by tactile stimulation of a wild-type sibling. (**Q**) Displacement of the trunk and tail during swimming in *ryr* mutants is smaller compared with that of wild-type siblings. For P and Q, the heads of embryos were pinned on a Sylgard dish leaving most of the trunk and tail free.

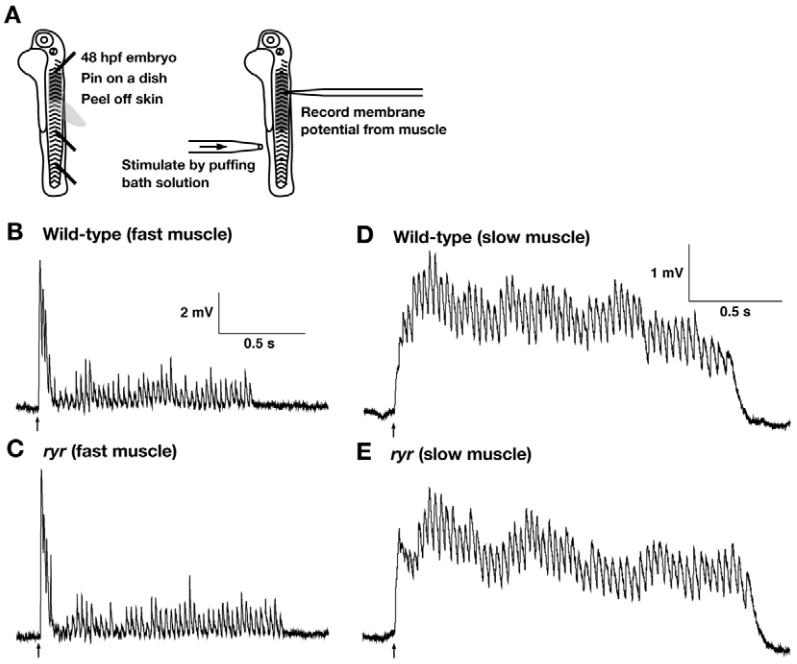

Fig. 2. The CNS and NMJ function normally in *ryr* mutants. (**A**) Schematic summary of the experimental procedure. Embryos (48 hpf) are pinned on a dish with tungsten wires through the notochord so as not to damage the CNS. The skin is peeled off to allow access to the muscle cells. Muscle voltage responses are evoked by mechanosensory stimulation delivered by a puff of bath solution to the tail and are recorded with a patch electrode. (**B**,**C**) Voltage recordings from fast muscle fibers of a wild-type sibling (B) and an *ryr* mutant (C) displayed similar patterns of depolarizations (fictive swimming). (**D**,**E**) Voltage recordings from slow muscle of a wild-type sibling (D) and an *ryr* mutant (E) display similar rhythmic depolarizations. Arrows indicate the time of stimulation.

trunk and tail free to move. The frequency of muscle contractions was comparable between wild-type siblings (38.7±5.2 Hz, n=10) and *ryr* embryos (35.9±4.5 Hz, n=10), but the amplitude of trunk and tail movements was significantly smaller in *ryr* mutants compared with wild-type siblings (Fig. 1P,Q). There were no obvious anatomical defects in *ryr* embryos and larvae, but mutants died at around 7-15 days post-fertilization (dpf), possibly from their inability to feed effectively. These observations suggest that weak contractions by trunk and tail muscles are the cause of slow swimming in *ryr*.

Output of the CNS is normal in *ryr* mutants

The fact that muscle contractions in *ryr* mutants were weaker than those in wild type suggested that the output from the CNS onto the muscle was decreased because of a defect in the CNS and/or NMJ, or that contractile responses of muscles were compromised due to a muscle defect. To see whether there was a decrease in signaling from the CNS and/or the NMJ, the voltage responses in muscles evoked by tactile stimulation were recorded (Fig. 2A). Voltage recordings from both wild-type-sibling and *ryr* mutant fast and slow muscles showed rhythmic depolarizations indicative of normal fictive swimming in response to touch (Fig. 2B-E). The amplitudes of the rhythmic depolarizations from wild-type-sibling and mutant fast muscles were comparable (wild type: 1.16±0.07 mV, n=4; *ryr*: 1.21±0.14 mV, n=4), as were the depolarizations in slow muscles (wild type: 1.02±0.25 mV, n=5; *ryr*: 0.90±0.17 mV, n=5). These results indicate that the CNS and the NMJ function normally in *ryr* mutants and suggest that they harbor a defect in muscles, downstream of the NMJ.

Ca^{2+} transient is smaller in *ryr* mutant fast muscle

Depolarization of the muscle membrane causes a transient increase in cytoplasmic Ca^{2+} mediated by E-C coupling that results in actin/myosin sliding and the contraction of muscle (Franzini-Armstrong and Protasi, 1997). Because muscles were defective in *ryr* mutants, we examined whether the increase in cytosolic Ca^{2+} was perturbed in mutant muscles by injecting live embryos with Ca^{2+} indicator dye, Calcium Green-1 dextran (Fig. 3A). The amplitude of Ca^{2+} transients in fast muscle was 3.3-times smaller in *ryr* mutants compared with wild-type siblings at 48 hpf [wild-type relative level of Calcium Green-1 fluorescence ($\Delta F/F$): 0.43±0.13, n=7; *ryr* $\Delta F/F$: 0.13±0.05, n=7; Student's t-test, $P<0.001$, Fig. 3B]. By contrast, Ca^{2+} transients in slow muscle were not perturbed in *ryr* mutants (wild-type $\Delta F/F$: 0.35±0.08, n=5; *ryr* $\Delta F/F$: 0.35±0.07, n=5; Fig. 3C). Furthermore, Ca^{2+} transients in mutants were comparable with wild-type siblings at 24 hpf (data not shown), when all mutants responded normally to tactile stimulation. Thus, a defect in E-C coupling in fast muscles appears to be the basis for weak contractions in *ryr* mutant muscles.

Proteins for E-C coupling are not clustered at t-tubule–SR junctions in *ryr* mutants

E-C coupling is mediated by direct interaction between DHPRs and RyRs, both of which are clustered at the juxtaposed membranes of t-tubule–SR junctions. To see how E-C coupling might be defective in mutant fast muscles, the distribution of RyRs and DHPRs were examined in *ryr* mutant muscles. Labeling with anti-RyR showed that RyRs were distributed in a striated pattern in wild-type fast muscles, which presumably represented the t-tubule–SR junctions (Fig. 4A), whereas RyR labeling was significantly reduced in mutant fast muscles (Fig. 4B). Similarly, anti-DHPRα1, anti-DHPRβ and anti-DHPRα2, respectively, showed that DHPRα1, DHPRβ and DHPRα2 were probably localized to t-tubule–SR junctions in wild-type fast muscles (Fig. 4C,E,G). Double labeling with anti-RyR and anti-DHPRα2 confirmed that RyRs and DHPRs were colocalized at presumptive t-tubule–SR junctions (Fig. 4I). On the other hand, DHPRα1, DHPRβ and DHPRα2 labeling were significantly reduced in mutant fast muscles (Fig. 4D,F,H,J). However, the distribution of RyRs and of DHPR subunits were unperturbed by the mutation in slow muscles (Fig. 4K-T). Electron micrographs verified the immunohistochemistry results. Patterned electron-dense structures that presumably represent juxtaposed RyRs and DHPRs were present at t-tubule–SR junctions in wild-type fast muscles (Fig. 4U) but not in *ryr* mutant fast muscles (Fig. 4V). The distribution of

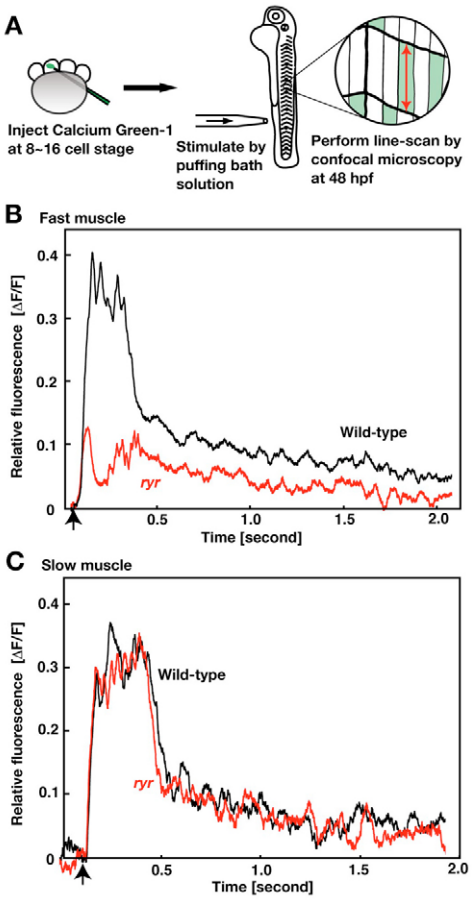

Fig. 3. Ca^{2+} transients are smaller in *ryr* mutant fast muscles. (**A**) Schematic summary of the experimental procedure. Calcium Green-1 dextran was injected into one cell of 8- to 16-cell-stage embryos. Embryos (48 hpf) were pinned on a dish and given mechanosensory stimulation by a puff of liquid to the tail. The relative level of Calcium Green-1 fluorescence (ΔF/F) in muscle fibers was assayed by line-scanning with a confocal microscopy. (**B**) The transient increase in relative fluorescence represents the transient increase of Ca^{2+} in the fast muscle following stimulation (arrow) of a wild-type embryo (black) and that of an *ryr* mutant (red). (**C**) The transient increase of Ca^{2+} in slow muscle is unperturbed in *ryr* mutants (red) compared to wild-type (black).

presumptive RyR/DHPR particles in slow muscles was comparable between wild type and *ryr* mutants (Fig. 4W,X). Thus, *ryr* mutants are deficient in E-C coupling in their fast muscles because of a lack of clustering by RyRs and DHPRs at the t-tubule–SR junctions.

The mutated gene in *ryr* mutants encodes RyR1

To identify the gene responsible for the *ryr* phenotype, the mutation was meiotically mapped to a region of chromosome 18 defined by two microsatellites, z737 (2.1 cM, 23 recombinants in 1110 meioses) and z8343 (6.9 cM, 77 recombinants in 1110 meioses) (Fig. 5A). A gene encoding for muscle ryanodine receptor 1 (*ryr1b*) was found in between these two markers in the Zv6 Ensemble assembly of the zebrafish genome. Furthermore, there was no recombination with a polymorphic marker in *ryr1b* (<0.09 cM, 0 recombinants in 1110 meioses). Thus, both genetic mapping and the RyR1 phenotype in mutants suggested that *ryr1b* was a good candidate for the *ryr* mutation. To see whether *ryr1b* was the *ryr* gene, *ryr1b* cDNA was cloned and sequenced from wild-type and mutant embryos. Wild-type *ryr1b* encodes 5076 amino acids (GenBank #AB247454, Fig. 5B). The *ryr1b* cDNA from *ryr* mutants contained a 32-bp insertion. This insertion generated a premature stop codon in the middle of the full-length protein that was 5′ to the sequences for the predicted transmembrane domains located at the C-terminus (Meissner, 1994). Reverse transcriptase (RT)-PCR with primers flanking the insertion was performed to confirm that the insertion was specifically found in *ryr* mutants (Fig. 5C). Both longer and shorter PCR fragments were amplified using the cDNA from a group of wild-type siblings as template (Fig. 5C, lane 1), whereas the longer fragment was predominant in mutants (Fig. 5C, lane 2). Only the shorter fragment was amplified from the cDNA of wild-type embryos of another strain, the AB strain, of zebrafish (Fig. 5C, lane 3), confirming that the shorter band corresponded to wild-type *ryr1b*. Sequencing of the longer and shorter fragments verified that the 32-bp insertion was found only in the longer product. Thus, the *ryr* phenotype is very likely to be due to mutation in *ryr1b*.

Genomic sequencing revealed that *ryr* mutants carry a 4046-bp DNA insertion, including the 32-bp cDNA insertion, in the intron between exon 48 and 49 of the *ryr1b* gene (Fig. 5D). Sequences flanking the 32 bp in the genomic insert contained splicing acceptor and donor sites, confirming that the 32-bp sequence acts as an additional exon in the mutant *ryr1b* gene. This genomic insertion might represent a transposable element, because it contained a repeated motif at both ends that are characteristic of Tc1/mariner family transposons (data not shown) (Ivics et al., 2004; Kawakami, 2005). Because the aberrant splicing results in a premature stop codon that predicts a truncated RyR1b lacking the channel domains, the great majority of fast muscle RyR1b would probably be non-functional.

To confirm whether a loss of RyR1b is responsible for the *ryr* phenotype, we attempted to phenocopy slow swimming by antisense knockdown of RyR1b and application of a specific inhibitor of RyR. We injected antisense morpholino oligonucleotides (MO1), which were complementary to the splice donor site of exon 48, into wild-type embryos and assayed touch responses at 36 hpf. MO1-injected wild-type embryos swam more slowly than control MO-injected wild-type embryos (MO-1 injected: 0.81±0.20 cm/s, n=12; control MO-injected: 1.78±0.35 cm/s, n=12; Student's t-test, P<0.001), much like mutant embryos. Interestingly, most of the MO1-injected embryos also exhibited weak coils of the trunk and tail following tactile stimulation at 24 hpf (82.0±7.8%, n≈43-76, five trials) rather than the normal fast, vigorous coils, suggesting that RyR1b is required for touch-induced coiling at earlier stages as well as for swimming at later stages. Correlated with the behavioral defects, the amount of *ryr1b* mRNA with normal splicing at 24, 36 and 48 hpf in MO1-injected embryos was reduced compared with control MO-injected embryos (Fig. 5E), confirming the efficacy of knockdown by MO1. Treatment of wild-type embryos with Ruthenium red, an inhibitor of RyR (Pessah et al., 1985), also phenocopied touch-induced slow swimming at 36 hpf (n=20). Thus, RyR1 is essential for normal muscle function in zebrafish, as it is in mammals.

The fact that weak muscle contractions in mutants were obvious after 36 hpf but not earlier than 30 hpf, whereas wild-type embryos in which *ryr1b* was knocked down exhibited weak contractions at 24 hpf, suggests that defective splicing was stage-dependent. To test this possibility, the head and trunk of individual embryos from a cross of two *ryr* carriers were subjected to genomic PCR and RT-PCR, respectively, to assay the genotype and splicing at 24 and 48 hpf (Fig. 5F). Wild-type embryos of the wt/wt genotype showed only a wild-type (short) RT-PCR fragment at both stages (Fig. 5F, lanes 1, 4), whereas wt/*ryr* embryos exhibited both wild-type (short)

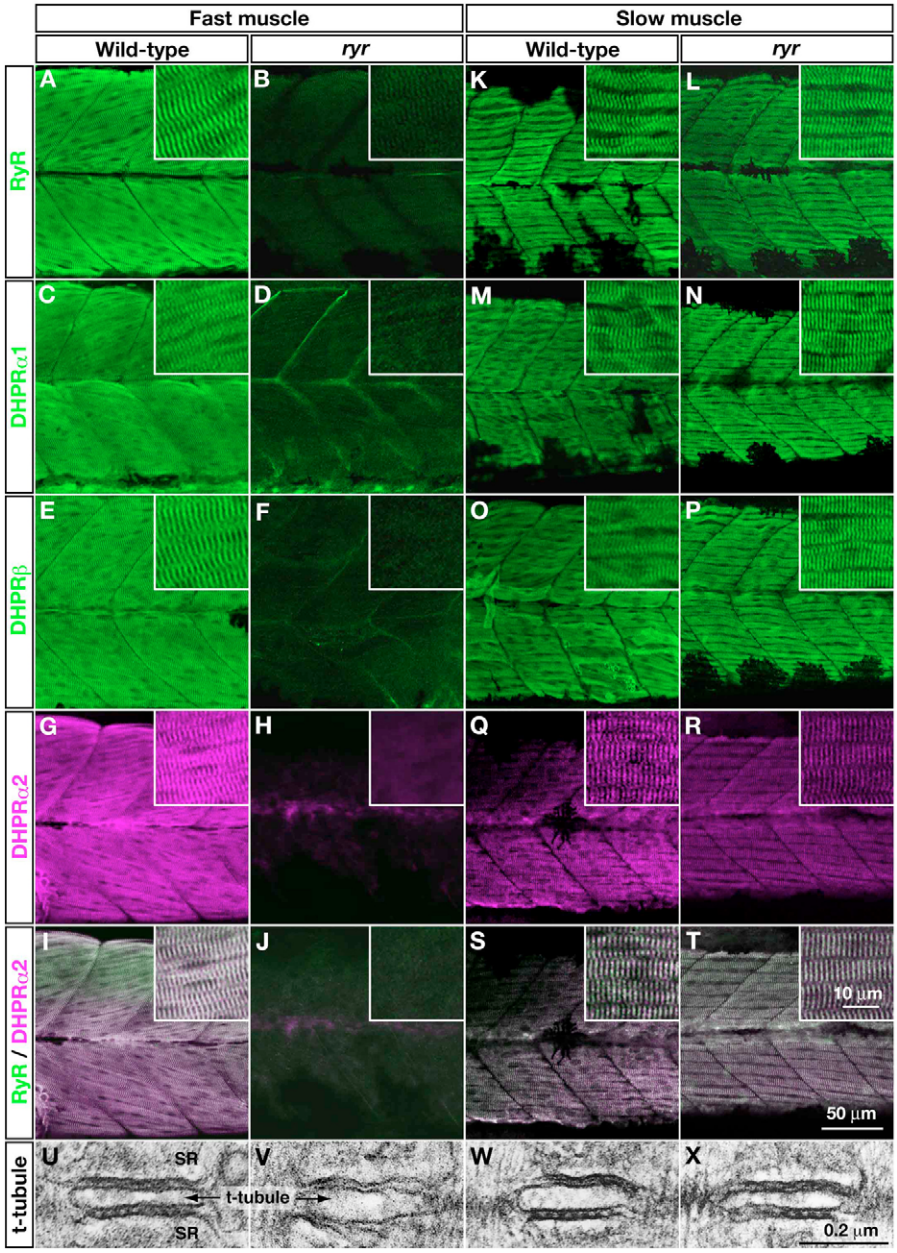

Fig. 4. E-C-coupling components are dramatically decreased in *ryr* fast muscles. (**A-H**,**K-R**) The distribution of RyRs and DHPRs were assayed in fast and slow muscles at 48 hpf with anti-RyR (A,B,K,L), anti-DHPRα1 (C,D,M,N), anti-DHPRβ (E,F,O,P) and anti-DHPRα2 (G,H,Q,R). Wild-type fast muscles express RyR (A), DHPRα1 (C), DHPRβ (E) and DHPRα2 (G) in a striated pattern that presumably corresponds to the t-tubule–SR junctions, whereas clustering is not observed in mutant fast muscles (B,D,F,H). Wild-type slow muscles express RyR (K), DHPRα1 (M), DHPRβ (O) and DHPRα2 (Q) in a striated pattern, as in wild-type fast muscles. *ryr* mutant slow muscles also express RyR (L), DHPRα1 (N), DHPRβ (P) and DHPRα2 (R) in a striated pattern. (**I**,**J**,**S**,**T**) RyR (green) and DHPRα2 (purple) are colocalized in wild-type fast (I) and slow (S) muscle and in mutant slow muscle (T) but not in *ryr* mutant fast muscle (J). Insets show a higher magnification of muscle fibers. (**U-X**) Electron micrographs of t-tubule–SR junctions in muscles at 48 hpf. Putative RyR-DHPR aggregates are visible as dense particles between t-tubule and SR membranes in wild-type fast muscle (U) but not in *ryr* mutant fast muscle (V). The RyR-DHPR aggregates are present in both wild-type (W) and mutant (X) slow muscles. SR, sarcoplasmic reticulum.

and mutant (long) fragments at both stages (Fig. 5F, lanes 2, 5). Mutant embryos (*ryr/ryr*) gave both wild-type and mutant fragments with comparable intensity at 24 hpf (Fig. 5F, lane 3), whereas the mutant product became predominant at 48 hpf (Fig. 5F, lane 6). These results suggest that the mutant behavioral phenotype was due to stage-dependent aberrant splicing in mutants.

The zebrafish genome contains potentially duplicated *ryr* genes

To identify other zebrafish genes encoding RyRs, we blasted the Zv6 Ensemble assembly of the zebrafish genome with protein sequences for human RYR1, RYR2 and RYR3, and found 14 genomic contigs that included sequences encoding for RyRs (Table 1). Each of the zebrafish RyR sequences were physically mapped with the LN54 radiation hybrid panel (Hukriede et al., 1999) and identified as RyR1, RyR2 or RyR3 based on homology with the human sequences. This classification suggested that there were at least five different ryanodine receptor genes in zebrafish: two for RyR1 [*ryr1a* in linkage group (LG)10 and *ryr1b* in LG18], two for RyR2 (*ryr2a* in LG12 and *ryr2b* in LG17) and one for RyR3 (*ryr3* in LG20).

ryr1b is expressed by fast muscle

Because *ryr* mutants were defective in E-C coupling in fast muscle, *ryr1b* should be expressed by fast muscles. RT-PCR showed that both *ryr1b* and *ryr1a* were expressed from 1 to 5 dpf as well as by the adult trunk (Fig. 6A). RT-PCR using cDNA from dissected adult fast muscles, however, showed that *ryr1b*, but not *ryr1a*, was expressed in fast muscle. In situ hybridization revealed that *ryr1b* was expressed by deep axial muscles probably representing fast muscles at 24 and 48 hpf (Fig. 6B-E). By contrast, expression of *ryr1a* was observed in superficial muscles under the skin, representing slow muscles (Devoto et al., 1996) (Fig. 6F-I). These results indicate that the potential duplicates of RyR1 were both expressed by muscles but that only RyR1b is expressed by fast muscles.

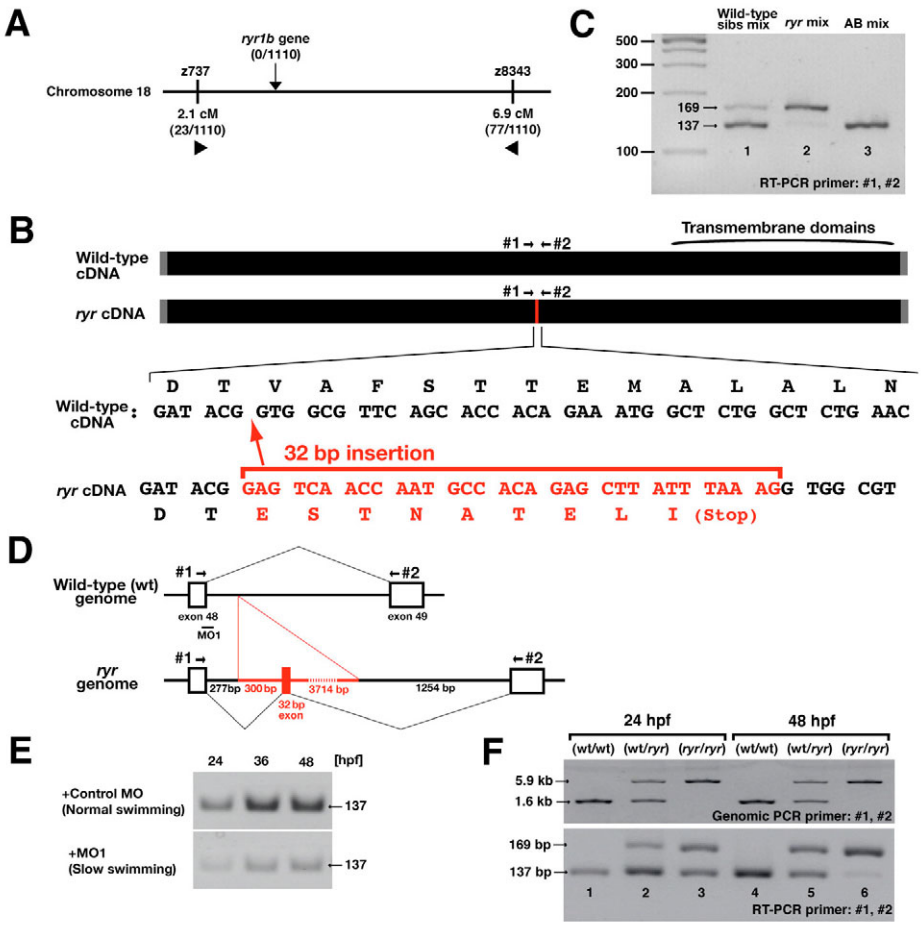

Fig. 5. *ryr* mutant embryos have a mutation in *ryr1b* due to a DNA insertion that leads to aberrant splicing of *ryr1b* mRNA. (**A**) Meiotic mapping placed the *ryr* locus between z737 and z8343 in chromosome 18. No recombination was found with a polymorphic marker in the *ryr1b* gene (0/1110). (**B**) *ryr* mutants contained a 32-bp insertion (red) in *ryr1b* mRNA that added a nonsense codon 5′ to the transmembrane domains. (**C**) Reverse transcriptase (RT)-PCR using primers #1 and #2 (see B) amplified both a longer mutant band (169 bp) and a shorter wild-type band (137 bp) from a group of wild-type siblings (lane 1), whereas the mutant band was predominant in *ryr* mutants (lane 2). The wild-type band can be seen faintly in the mutant lane. Only the shorter band was amplified from wild-type AB embryos (lane 3). (**D**) *ryr* mutants carry a 4046-bp insertion (red) in the intron between exons 48 and 49 of *ryr1b* that includes the additional 32-bp sequence found in the mutant cDNA. (**E**) Injection of an antisense morpholino (MO1, see D) into recently fertilized wild-type embryos effectively decreases normal *ryr1b* mRNA at 24, 36 and 48 hpf, whereas control MO does not. A fragment of normal *ryr1b* mRNA was examined by RT-PCR with primers #1 and #2 (see D). (**F**) Genomic PCR and RT-PCR with primers #1 and #2 using individual embryos as a template. Genotypes, as shown, were identified by genomic PCR. Notice that, in mutants, the intensity of the wild-type (short) band amplified by RT-PCR was comparable to that of the mutant (long) band at 24 hpf (lane 3) but was diminished at 48 hpf (lane 6).

The *ryr* mutant is a disease model of MmD

MmD, a recessive myopathy, is caused by RYR1 mutations in human and is pathologically defined by multiple amorphous cores in muscle fibers (Engel, 1967; Jungbluth et al., 2004). To examine whether *ryr* mutants displayed morphological defects in muscle, transverse sections of larval axial muscles were analyzed by transmission electron microscopy. Superficial slow muscles appeared comparable between wild type and mutant (data not shown). Well-formed actin/myosin bundles and SR were observed in wild-type fast muscle at 2, 7 and 14 dpf (Fig. 7A-C). Mutant fast muscle, however, displayed small amorphous cores (50-100 nm in diameter) at 2 dpf (Fig. 7D). The diameter of the cores in mutant fast muscles increased with development (50-500 nm at 7 dpf; 100-800 nm at 14 dpf; Fig. 7E,F). Disorganization of the SR was also evident at 7 dpf and, in some cases, the SR was missing at 14 dpf. Thus, *ryr* mutant fast muscles displayed ultrastructural defects similar to those seen in MmD muscles.

Because the *ryr* mutation was due to defective splicing of *ryr1b* mRNA, we wondered whether normal swimming could be restored by preventing aberrant splicing. This treatment was examined by injection of antisense morpholino oligonucleotides (MO2) against the splice acceptor site of the 32-bp insert into recently fertilized progeny of *ryr* carriers (Fig. 7G). After testing their response to tactile stimulation at 36 hpf, the head and trunk of embryos were subjected to genomic PCR and RT-PCR, respectively, to assay genotype and splicing (Fig. 7H). Injection of control MO had no effect either on swimming or on splicing (Fig. 7H, lanes 1-3). MO2-injected wt/wt embryos exhibited normal swimming and expressed only the wild-type, short fragment (Fig. 7H, lane 4). MO2-injected wt/*ryr* embryos exhibited normal swimming and expressed both the normal (short) and mutant (long) fragments (Fig. 7H, lane 5). However, 49% (23/47) of MO2-injected *ryr/ryr* embryos exhibited recovery (>1.0 cm/s) in swimming (MO2 injected: 1.34±0.32 cm/s; control MO-injected: 0.74±0.22 cm/s; Student's *t*-test, $P<0.001$).

Table 1. Zebrafish has five ryanodine receptor genes

Zv6 genomic contig	LG	LOD score	Gene
Zv6_LG10_scaffold1488_BX088525	10	15.9	*ryanodine receptor 1a* (slow muscle)
Zv6_LG10_scaffold1488_BX323802	10	15.9	
Zv6_LG18_scaffold2701	18	15.5	*ryanodine receptor 1b* (fast muscle)
Zv6_LG18_scaffold2704	18	13.3	
Zv6_NA1631	18	12.0	
Zv6_LG10_scaffold1543	18	17.9	
Zv6_LG12_scaffold1783	12	15.0	*ryanodine receptor 2a*
Zv6_NA172	12	14.6	
Zv6_LG12_scaffold2517_BX323986	17	17.6	*ryanodine receptor 2b*
Zv6_LG12_scaffold2525_BX005070	17	17.6	
Zv6_LG12_scaffold2444	17	18.6	
Zv6_LG12_scaffold2462	17	18.4	
Zv6_NA2171	17	18.4	
Zv6_LG20_scaffold2945_BX682544	20	9.8	*ryanodine receptor 3*

A blast search of the zebrafish genomic database (Zv6 Ensemble) with protein sequences of human ryanodine receptor 1, 2 and 3 identified 14 different genomic contigs containing partial sequence similar to human ryanodine receptors. Each genomic contig was physically mapped by probing the LN54 radiation hybrid panel to one of five different loci. The LOD score indicates reliability of physical mapping with scores higher than 5 considered reliable. LG, linkage group; LOD, log of odds.

They expressed an increase in the proportion of wild-type, short mRNA to mutant, long mRNA (Fig. 7H, lanes 6, 7) compared with that in control MO-injected *ryr/ryr* embryos (Fig. 7H, lane 3). By contrast, MO2-injected mutant embryos that exhibited slow swimming (<1.0 cm/s, 51%, 24/47) predominantly expressed the mutant, long fragment, with little normal product (Fig. 7H, lanes 8, 9) much like control MO-injected mutants (Fig. 7H, lane 3).

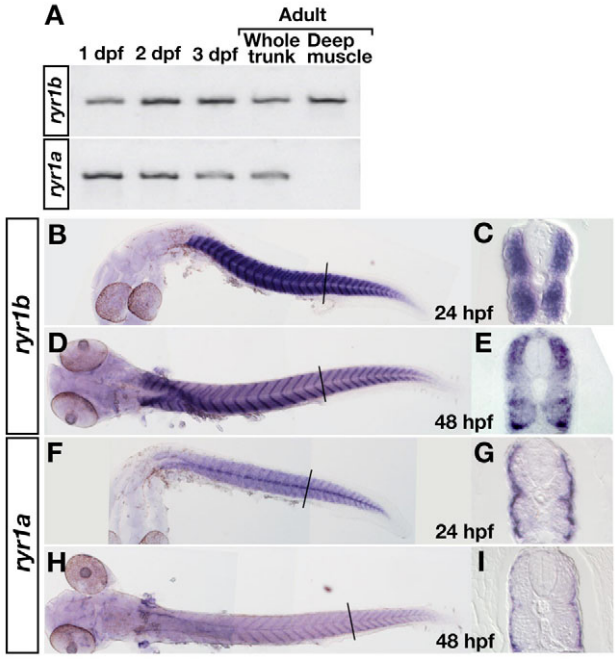

Fig. 6. *ryr1b* and *ryr1a* are expressed by fast and slow muscle, respectively. (**A**) Reverse transcriptase (RT)-PCR shows that both *ryr1b* and r*yr1a* are expressed at 1, 2 and 3 dpf, and in adults. RT-PCR with mRNA from deep muscles indicates that *ryr1b* but not *ryr1a* is expressed by adult fast muscles. (**B-I**) In situ hybridization with *ryr1b* (B-E) and *ryr1a* (F-I) probes. Wholemounts show that both genes are expressed by muscle at 24 (B,F) and 48 (D,H) hpf. Cross-sections show that *ryr1b* is expressed by deep, fast muscles (C,E), whereas *ryr1a* is expressed by superficial, slow muscles but not by fast muscles (G,I).

However, rescue of swimming was transient, because the 23 embryos that exhibited recovery at 36 hpf exhibited slow swimming by 60 hpf, presumably due to breakdown of the MO. These MO2-injected mutants died at around 7-15 dpf, much like uninjected *ryr* mutants. Furthermore, electron micrographs of the fast muscles of MO2-injected *ryr* mutants displayed amorphous cores in fast muscle at 7 dpf (n=4, data not shown). Similar results were obtained with another antisense morpholino oligonucleotides (MO3) that was complementary to the donor splice site of the 32-bp insert (data not shown). Thus, prevention of aberrant splicing with antisense MO treatment can transiently restore normal swimming, confirming that the aberrant splicing is responsible for the *ryr* phenotype. It also indicates that *ryr* mutants might be useful for examining antisense-mediated treatment in vivo.

DISCUSSION

ryr mutants have an E-C-coupling defect in fast muscles

Several findings demonstrate that *ryr* mutants exhibit weak muscle contractions due to an E-C-coupling defect in fast muscles. First, depolarization of the muscle membrane evoked by output from the CNS was normal in *ryr* fast muscles. Second, Ca^{2+} transients following the depolarization of muscles were decreased in *ryr* fast muscles. Third, there was a dramatic decrease in E-C-coupling components, such as RyRs and DHPRs, at the t-tubules–SR junctions in *ryr* fast muscles. Indeed, most of the *ryr1b* transcripts were aberrantly spliced in the mutants, leading to a hypomorphic condition due to reduced synthesis of normal mRNA. Therefore, a reduction of RyR1b in fast muscles leads to a decrease in DHPR and RyR at the t-tubule–SR junctions and to a decrease in Ca^{2+} released from the SR into the cytosol, leading to weak muscle contractions in *ryr* mutants.

The zebrafish immotile mutant, *relaxed* (also known as *cacnb1* – Zebrafish Information Network), is deficient in E-C coupling because of a null mutation in DHPRβ1 (Schredelseker et al., 2005; Zhou et al., 2006). In *relaxed* mutant muscles, DHPRα1 was significantly reduced, but RyR1 was correctly targeted to the t-tubule–SR junctions. In *ryr* mutants, by contrast, there was a dramatic decrease in both DHPR and RyR1 even when the t-tubules and the SR were not damaged. Taken together, the phenotypes of the two zebrafish mutations corroborate the finding that the formation

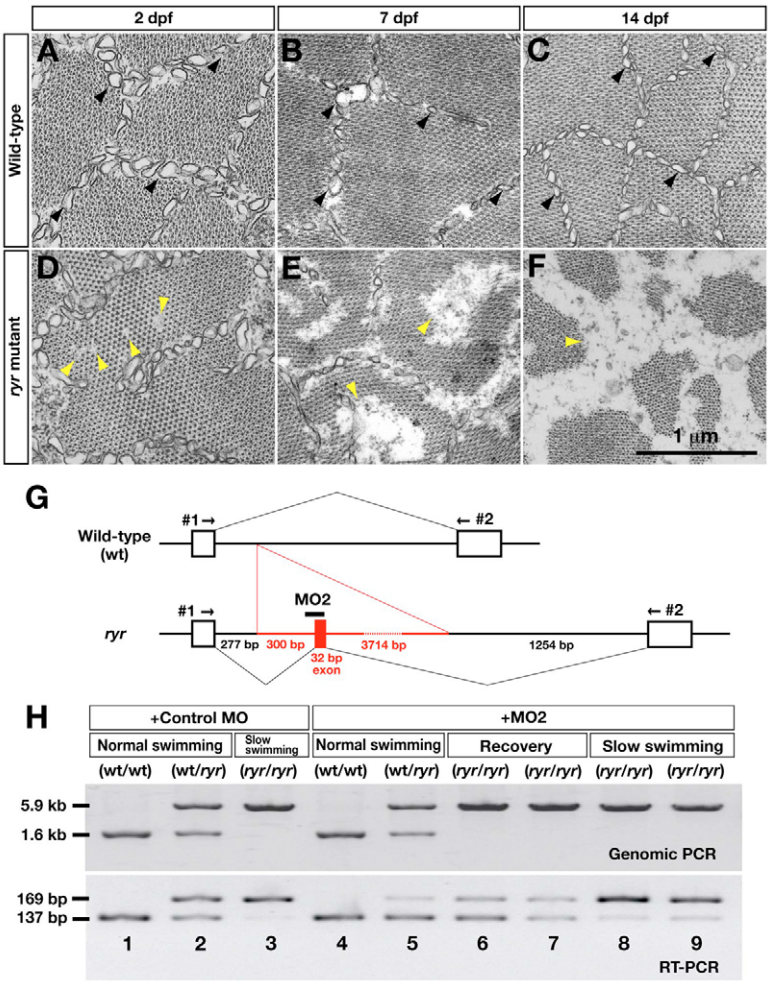

Fig. 7. *ryr* mutants exhibit a minicore phenotype similar to that observed in MmD and the behavioral phenotype can be rescued by preventing aberrant splicing of *ryr1b* mRNA. (**A-C**) Electron micrographs of wild-type fast muscles showing sarcoplasmic reticulum (SR; black arrowheads), and bundles of actin and myosin at 2, 7 and 14 dpf. (**D-F**) Amorphous cores are seen in *ryr* mutants (yellow arrowheads). Diameters of the cores are 50-100 nm, 50-500 nm and 100-800 nm at 2, 7 and 14 dpf, respectively. The SR is disorganized at 7 dpf and missing at 14 dpf. (**G**) The behavioral defects of *ryr* mutants are treatable by an antisense morpholino that blocks abnormal splicing of *ryr1b* mRNA. A diagram showing the wild-type and mutant *ryr1b* genes with the location of the morpholino (MO2) that was designed against the splice acceptor site of the aberrant exon of the mutant gene is shown. (**H**) Control MO (lanes 1-3) or MO2 (lanes 4-9) was injected into the progeny of an *ryr* carrier incross. Swimming of injected embryos was examined at 36 hpf, and the head and trunk of individual embryos were subjected to genomic PCR and RT-PCR, respectively. Control MO-injected wt/wt embryos exhibited normal swimming and expressed only the wild-type, short fragment by RT-PCR (lane 1). Control MO-injected wt/*ryr* embryos exhibited normal swimming and expressed both the wild-type short and the mutant long fragments (lane 2). Control MO-injected *ryr/ryr* embryos exhibited slow swimming and predominantly expressed the mutant fragment (lane 3). MO2-injected wt/wt embryos exhibited normal swimming and expressed only the wild-type, short fragment (lane 4). MO2-injected wt/*ryr* embryos exhibited normal swimming and expressed both fragments (lane 5). In mutant embryos (*ryr/ryr*) showing recovery of swimming, normal splicing (short band) was increased (lanes 6, 7 compared to lane 3). On the other hand, in mutants that exhibited slow swimming, the proportion of wild-type mRNA was much lower (lanes 8, 9) compared to mutants that exhibited recovery (lanes 6, 7).

of DHPR tetrads requires the presence of RyR1 (Takekura et al., 1995). Indeed, a cytoplasmic domain of RyR1 is essential for the physical interaction with an intracellular loop of DHPRα1 in cultured mammalian myotubes (Kugler et al., 2004; Proenza et al., 2002). The failure of DHPR to localize to the t-tubule–SR junctions is probably a direct consequence of the failure of RyR1b to be targeted to the SR in *ryr* mutants.

ryr1b is the *ryr* gene

In *ryr* mutants, we found a 32-bp insertion in most of the *ryr1b* transcripts, which resulted in the generation of a nonsense codon. The 32-bp exon was included in a 4046-bp DNA insertion in the mutant *ryr1b* gene. This large insertion might be derived from a transposable element in zebrafish. Indeed, sequencing of the insertion revealed inverted repeats characteristic of the Tc1/mariner family of transposons (Ivics et al., 2004; Kawakami, 2005). Although *ryr1b* was expressed by fast muscles at 24 hpf and was essential for E-C coupling at later stages, *ryr* mutants responded to touch with normal C-bends at 24 hpf and exhibited slow swimming after 36 hpf. This lack of a mutant phenotype at 24 hpf can be explained by the possibility that splicing of *ryr1b* might be developmentally regulated and that the aberrant splicing may only occur during later stages. In fact, half of the *ryr1b* transcripts were normally processed at 24 hpf, whereas most *ryr1b* mRNA transcripts were aberrantly spliced at 48 hpf. A splicing factor, which determines exon preference, might be differentially regulated between 1 and 2 dpf. The finding that knockdown of RyR1b translation in wild-type embryos leads to weak muscle contractions at 24 hpf is consistent with this hypothesis.

We found that zebrafish have two genes encoding RyR1; *ryr1a* expressed by slow muscles and *ryr1b* by fast muscles. A similar division of labor between duplicated RyR1s in slow and fast muscles appears in other fish, such as blue marlin (*Makaira nigricans*) and yellowfin tuna (*Thunnus albacares*) (Franck et al., 1998; Morrissette et al., 2000; Morrissette et al., 2003). Although single-channel analysis indicates that channel activity of RyR1 in fast muscle is higher than that in slow muscle (Morrissette et al., 2000), any functional difference in E-C coupling has not been examined. It would be interesting to examine potential differences in E-C coupling between slow and fast muscles to see how the requirements of the two muscle types dictate divergent RyR1s and how these differences may have evolved.

The *ryr* mutant is an animal model for MmD

The zebrafish *ryr* mutant phenotype shares several crucial features with human MmD. First, mutations in genes encoding RyR1 are responsible for both the *ryr* phenotype and MmD. Second, both the *ryr* phenotype and MmD are inherited as autosomal recessives. Third, both *ryr* mutants and individuals with MmD exhibit muscle weakness. Fourth, both *ryr* mutants and individuals with Mmd display myopathy characterized by minicores in histological sections. The amorphous cores in MmD (2-25 μm in diameter) are

associated with labeling for reductase activity in mitochondria with NADH-TR (tetrazolium reductase) (Engel, 1967; Martin et al., 1986; Swash and Schwartz, 1981). Unfortunately, NADH-TR staining appears to not be useful in fish (Johnston et al., 1975; Matsuoka and Iwai, 1984). However, electron microscopy clearly demonstrated amorphous cores in zebrafish *ryr* mutant muscles and showed that they are evident in embryonic muscles. The fact that RyR1-deficient mice die on the day of birth limits their usefulness as an animal model of MmD (Takeshima et al., 1994). By contrast, zebrafish *ryr* mutants die 7-15 dpf, but their fast development and accessibility might be useful for detailed physiological and pathological analysis of the consequences of MmD.

We succeeded in treating muscle weakness in *ryr* mutants by the application of an antisense morpholino that increased the normal splicing of *ryr1b* and restored normal swimming. Germane to our finding, antisense-mediated exon skipping restored normal dystrophin expression in certain dystrophin mutant mice and in cultured muscle cells from Duchenne muscular dystrophy individuals harboring splicing defects (Goyenvalle et al., 2004; van Deutekom et al., 2001). This novel therapeutic strategy might represent an effective treatment for the human genetic disease and is under clinical trials (Muntoni et al., 2005; Wilton and Fletcher, 2006). Interestingly, Monnier and her colleagues reported a hypomorph in human RYR1 that was responsible for MmD (Monnier et al., 2003), similar to the zebrafish *ryr* mutants. In this case, an aberrant splice donor site was generated by a point mutation in an intron, resulting in incorrect splicing and in the generation of a nonsense codon in most of the human RYR1 transcripts. Given the similarity to *ryr* mutants, this case of MmD might be treated by blocking aberrant splicing with antisense reagents.

We thank Richard I. Hume (University of Michigan) and Yoichi Oda (Nagoya University) for helpful discussion and generous use of electrophysiology equipment. We also thank Koichi Kawakami (National Institute of Genetics), Ikuya Nonaka (Musashi Hospital, National Center of Neurology and Psychiatry) and Tokuko Niwa (Nagoya University) for discussion, technical suggestion and fish care, respectively. This work was supported by a Grant-in-Aid for Scientific Research on Priority Areas 'System Genomics' and 'Glia-Neuron Network' and by a Grant-in-Aid for Young Scientists (A) from the Ministry of Education, Culture, Sports, Science and Technology of Japan and the Hori Information Science Promotion Foundation, the Brain Science Foundation, the Life Science Foundation, the Narishige Neuroscience Research Foundation, the Sumitomo Foundation, the Kowa Life Science Foundation, the Mochida Memorial Foundation for Medical and Pharmaceutical Research and the Goho Life Sciences International Fund. Supported by grants from the NINDS to J.Y.K. J.H. was supported by a Research Fellowship of the Japan Society for Promotion of Science for Young Scientists. L.S.-A. was partly supported by a Fellowship from FRSQ. H.H. was supported by Long Term Fellowship of the International Human Frontier Science Program Organization.

Supplementary material

Supplementary material for this article is available at http://dev.biologists.org/cgi/content/full/134/15/2771/DC1

References

Airey, J. A., Beck, C. F., Murakami, K., Tanksley, S. J., Deerinck, T. J., Ellisman, M. H. and Sutko, J. L. (1990). Identification and localization of two triad junctional foot protein isoforms in mature avian fast twitch skeletal muscle. *J. Biol. Chem.* **265**, 14187-14194.

Bahary, N., Davidson, A., Ransom, D., Shepard, J., Stern, H., Trede, N., Zhou, Y., Barut, B. and Zon, L. I. (2004). The Zon laboratory guide to positional cloning in zebrafish. *Methods Cell Biol.* **77**, 305-329.

Bassett, D. I. and Currie, P. D. (2003). The zebrafish as a model for muscular dystrophy and congenital myopathy. *Hum. Mol. Genet.* **12**, R265-R270.

Block, B. A., Imagawa, T., Campbell, K. P. and Franzini-Armstrong, C. (1988). Structural evidence for direct interaction between the molecular components of the transverse tubule/sarcoplasmic reticulum junction in skeletal muscle. *J. Cell Biol.* **107**, 2587-2600.

Buss, R. R. and Drapeau, P. (2000). Physiological properties of zebrafish embryonic red and white muscle fibers during early development. *J. Neurophysiol.* **84**, 1545-1557.

Buss, R. R. and Drapeau, P. (2001). Synaptic drive to motoneurons during fictive swimming in the developing zebrafish. *J. Neurophysiol.* **86**, 197-210.

Catterall, W. A. (2000). Structure and regulation of voltage-gated Ca^{2+} channels. *Annu. Rev. Cell Dev. Biol.* **16**, 521-555.

Cheung, A., Dantzig, J. A., Hollingworth, S., Baylor, S. M., Goldman, Y. E., Mitchison, T. J. and Straight, A. F. (2002). A small-molecule inhibitor of skeletal muscle myosin II. *Nat. Cell Biol.* **4**, 83-88.

Devoto, S. H., Melançon, E., Eisen, J. S. and Westerfield, M. (1996). Identification of separate slow and fast muscle precursor cells in vivo, prior to somite formation. *Development* **122**, 3371-3380.

Drapeau, P., Saint-Amant, L., Buss, R. R., Chong, M., McDearmid, J. R. and Brustein, E. (2002). Development of the locomotor network in zebrafish. *Prog. Neurobiol.* **68**, 85-111.

Eaton, R. C. and Farley, R. D. (1973). Development of the mauthner neurons in embryos and larvae of the zebrafish, *Brachydanio rerio*. *Copeia* **4**, 673-682.

Engel, W. K. (1967). Muscle biopsies in neuromuscular diseases. *Pediatr. Clin. North Am.* **14**, 963-995.

Fetcho, J. R. (1992). The spinal motor system in early vertebrates and some of its evolutionary changes**.** *Brain Behav. Evol.* **40,** 82-97**.**

Fetcho, J. R. (2006). The utility of zebrafish for studies of the comparative biology of motor systems. *J. Exp. Zoolog. B Mol. Dev. Evol.* doi: 10.1002/jez.b.21127. I**n press**.

Fetcho, J. R. and Bhatt, D. H. (2004). Genes and photons: new avenues into the neuronal basis of behavior. *Curr. Opin. Neurobiol.* **14**, 707-714.

Fill, M. and Copello, J. A. (2002). Ryanodine receptor calcium release channels. *Physiol. Rev.* **82**, 893-922.

Flucher, B. E., Obermair, G. J., Tuluc, P., Schredelseker, J., Kern, G. and Grabner, M. (2005). The role of auxiliary dihydropyridine receptor subunits in muscle. *J. Muscle Res. Cell Motil.* **26**, 1-6.

Franck, J. P. C., Morrissette, J., Keen, J. E., Londraville, R. L., Beamsley, M. and Block, B. A. (1998). Cloning and characterization of fiber type-specific ryanodine receptor isoforms in skeletal muscles of fish. *Am. J. Physiol. Cell Physiol.* **275**, C401-C415.

Franzini-Armstrong, C. and Protasi, F. (1997). Ryanodine receptors of striated muscles: a complex channel capable of multiple interactions. *Physiol. Rev.* **77**, 699-729.

Gahtan, E., Sankrithi, N., Campos, J. B. and O'Malley, D. M. (2002). Evidence for a widespread brain stem escape network in larval zebrafish. *J. Neurophysiol.* **87**, 608-614.

Gates, M. A., Kim, L., Egan, E. S., Cardozo, T., Sirotkin, H. I., Dougan, S. T., Lashkari, D., Abagyan, R., Schier, A. F. and Talbot, W. S. (1999). A genetic linkage map for zebrafish: comparative analysis and localization of genes and expressed sequences. *Genome Res.* **9**, 334-347.

Goyenvalle, A., Vulin, A., Fougerousse, F., Leturcq, F., Kaplan, J.-C., Garcia, L. and Danos, O. (2004). Rescue of dystrophic muscle through U7 snRNA-mediated exon skipping. *Science* **306**, 1796-1799.

Granato, M., van Eeden, F. J. M., Schach, U., Trowe, T., Brand, M., Furutani-Seiki, M., Haffter, P., Hammerschmidt, M., Heisenberg, C.-P., Jiang, Y.-J. et al. (1996). Genes controlling and mediating locomotion behavior of the zebrafish embryo and larva. *Development* **123**, 399-413.

Hatakeyama, J., Bessho, Y., Katoh, K., Ookawara, S., Fujioka, M., Guillemot, F. and Kageyama, R. (2004). *Hes* genes regulate size, shape and histologenesis of the nervous system by control of the timing of neural stem cell differentiation. *Development* **131**, 5539-5550.

Hirata, H., Saint-Amant, L., Waterbury, J., Cui, W. W., Zhou, W., Li, Q., Goldman, D., Granato, M. and Kuwada, J. Y. (2004). *accordion*, a zebrafish behavioral mutant, has a muscle relaxation defect due to a mutation in the ATPase Ca^{2+} pump SERCA1. *Development* **131**, 5457-5468.

Hirata, H., Saint-Amant, L., Downes, G. B., Cui, W. W., Zhou, W., Granato, M. and Kuwada, J. Y. (2005). Zebrafish *bandoneon* mutants display behavioral defects due to a mutation in the glycine receptor β-subunit. *Proc. Natl. Acad. Sci. USA* **102**, 8345-8350.

Hukriede, N. A., Joly, L., Tsang, M., Miles, J., Tellis, P., Epstein, J. A., Barbazuk, W. B., Li, F. N., Paw, B., Postlethwait, J. H. et al. (1999). Radiation hybrid mapping of the zebrafish genome. *Proc. Natl. Acad. Sci. USA* **96**, 9745-9750.

Ivics, Z., Kaufman, C. D., Zayed, H., Miskey, C., Walisko, O. and Izsvák, Z. (2004). The *sleeping beauty* transposable element: evolution, regulation and genetic applications. *Curr. Issues Mol. Biol.* **6**, 43-56.

Johnston, I. A., Ward, P. S. and Goldspink, G. (1975). Studies on the swimming musculature of the rainbow trout. I. Fiber types. *J. Fish Biol.* **7**, 451-458.

Jungbluth, H., Beggs, A., Bönnemann, C., Bushby, K., Groote, C. C., Estournet-Mathiaud, B., Goemans, N., Guicheney, P., Lescure, A., Lunardi, J. et al. (2004). 111th ENMC international workshop on multi-minicore disease. *Neuromuscul. Disord.* **14**, 754-766.

Kawakami, K. (2005). Transposon tools and methods in zebrafish. *Dev. Dyn.* **234**, 244-254.

Kugler, G., Weiss, R. G., Flucher, B. E. and Grabner, M. (2004). Structural

requirements of the dihydropyridine receptor α_{1S} II-III loop for skeletal-type excitation-contraction coupling. *J. Biol. Chem.* **279**, 4721-4728.
Kunkel, L. M., Bachrach, E., Bennett, R. R., Guyon, J. and Steffen, L. (2006). Diagnosis and cell-based therapy for Duchenne muscular dystrophy in humans, mice and zebrafish. *J. Hum. Genet.* **51**, 397-406.
Leung, A. T., Imagawa, T., Block, B., Franzini-Armstrong, C. and Campbell, K. P. (1988). Biochemical and ultrastructural characterization of the 1,4-dihydropyridine receptor from rabbit skeletal muscle. *J. Biol. Chem.* **263**, 994-1001.
Lieschke, G. J. and Currie, P. D. (2007). Animal models of human disease: zebrafish swim into view. *Nat. Rev. Genet.* **8**, 353-367.
Lyfenko, A. D., Goonasekera, S. A. and Dirksen, R. T. (2004). Dynamic alterations in myoplasmic Ca^{2+} in malignant hyperthermia and central core disease. *Biochem. Biophys. Res. Commun.* **322**, 1256-1266.
MacLennan, D. H. and Phillips, M. S. (1992). Malignant hyperthermia. *Science* **256**, 789-794.
Martin, J. J., Bruyland, M., Busch, H. F. M., Farriaux, J. P., Krivosic, I. and Ceuterick, C. (1986). Plecore disease. *Acta Neuropathol.* **72**, 142-149.
Matsuoka, M. and Iwai, T. (1984). Development of the myotomal musculature in the red sea bream. *Bull. Jpn. Soc. Sci. Fish.* **50**, 29-35.
Meissner, G. (1994). Ryanodine receptor/Ca^{2+} release channels and their regulation by endogenous effectors. *Annu. Rev. Physiol.* **56**, 485-508.
Monnier, N., Ferreiro, A., Marty, I., Labarre-Vila, A., Mezin, P. and Lunardi, J. (2003). A homozygous splicing mutation causing a depletion of skeletal muscle RYR1 is associated with multi-minicore disease congenital myopathy with ophthalmoplegia. *Hum. Mol. Genet.* **12**, 1171-1178.
Morrissette, J., Xu, L., Nelson, A., Meissner, G. and Block, B. A. (2000). Characterization of RyR1-slow, a ryanodine receptor specific to slow-twitch skeletal muscle. *Am. J. Physiol. Regul. Integr. Comp. Physiol.* **279**, R1889-R1898.
Morrissette, J. M., Franck, J. P. G. and Block, B. A. (2003). Characterization of ryanodine receptor and Ca^{2+}-ATPase isoforms in the thermogenic heater organ of blue marlin (*Makaira nigricans*). *J. Exp. Biol.* **206**, 805-812.
Morton, M. E. and Froehner, S. C. (1987). Monoclonal antibody identifies a 200-kDa subunit of the dihydropyridine-sensitive calcium channel. *J. Biol. Chem.* **262**, 11904-11907.
Morton, M. E. and Froehner, S. C. (1989). The α_1 and α_2 polypeptides of the dihydropyridine-sensitive calcium channel differ in developmental expression and tissue distribution. *Neuron* **2**, 1499-1506.
Muntoni, F., Bushby, K. and van Ommen, G. (2005). 128th ENMC international workshop on 'preclinical optimization and phase I/II clinical trials using antisense oligonucleotides in Duchenne muscular dystrophy' 22-24 October 2004, Naarden, the Netherlands. *Neuromuscul. Disord.* **15**, 450-457.
Nasevicius, A. and Ekker, S. C. (2000). Effective targeted gene 'knockdown' in zebrafish. *Nat. Genet.* **26**, 216-220.
Nüsslein-Volhard, C. and Dahm, R. (2002). *Zebrafish.* New York: Oxford University Press.
Pessah, I. N., Waterhouse, A. L. and Casida, J. E. (1985). The calcium-ryanodine receptor complex of skeletal and cardiac muscle. *Biochem. Biophys. Res. Commun.* **128**, 449-456.
Proenza, C., O'Brien, J., Nakai, J., Mukherjee, S., Allen, P. D. and Beam, K. G. (2002). Identification of a region of RyR1 that participates in allosteric coupling with the α_{1S} ($Ca_v1.1$) II-III loop. *J. Biol. Chem.* **277**, 6530-6535.
Saint-Amant, L. and Drapeau, P. (1998). Time course of the development of motor behaviors in the zebrafish embryo. *J. Neurobiol.* **37**, 622-632.
Schredelseker, J., Biase, V. D., Obermair, G. J., Felder, E. T., Flucher, B. E., Franzini-Armstrong, C. and Grabner, M. (2005). The β_{1a} subunit is essential for the assembly of dihydropyridine-receptor arrays in skeletal muscle. *Proc. Natl. Acad. Sci. USA* **102**, 17219-17224.
Shimoda, N., Knapik, E. W., Ziniti, J., Sim, C., Yamada, E., Kaplan, S., Jackson, D., de Sauvage, F., Jacob, H. and Fishman, M. C. (1999). Zebrafish genetic map with 2000 microsatellite markers. *Genomics* **58**, 219-232.
Swash, M. and Schwartz, M. S. (1981). Familial multicore disease with focal loss of cross-striations and ophthalmoplegia. *J. Neurol. Sci.* **52**, 1-10.
Takekura, H., Nishi, M., Noda, T., Takeshima, H. and Franzini-Armstrong, C. (1995). Abnormal junctions between surface membrane and sarcoplasmic reticulum in skeletal muscle with a mutation targeted to the ryanodine receptor. *Proc. Natl. Acad. Sci. USA* **92**, 3381-3385.
Takeshima, H., Nishimura, S., Matsumoto, T., Ishida, H., Kangawa, K., Minamino, N., Matsuo, H., Ueda, M., Hanaoka, M., Hirose, T. et al. (1989). Primary structure and expression from complementary DNA of skeletal muscle ryanodine receptor. *Nature* **339**, 439-445.
Takeshima, H., Iino, M., Takekura, H., Nishi, M., Kuno, J., Minowa, O., Takano, H. and Noda, T. (1994). Excitation-contraction uncoupling and muscular degeneration in mice lacking functional skeletal muscle ryanodine-receptor gene. *Nature* **369**, 556-559.
van Deutekom, J. C. T., Bremmer-Bout, M., Janson, A. A. M., Ginjaar, I. B., Baas, F., den Dunnen, J. T. and van Ommen, G.-J. B. (2001). Antisense-induced exon skipping restores dystrophin expression in DMD patient derived muscle cells. *Hum. Mol. Genet.* **10**, 1547-1554.
Wen, H. and Brehm, P. (2005). Paired motor neuron-muscle recordings in zebrafish test the receptor blockade model for shaping synaptic current. *J. Neurosci.* **25**, 8104-8111.
Westerfield, M. (2000). *The Zebrafish Book. A Guide for the Laboratory use of Zebrafish (Danio rerio)* (4th edn). Eugene: University of Oregon Press.
Wilson, S. W., Brand, M. and Eisen, J. S. (2002). Patterning the zebrafish central nervous system. *Results Probl. Cell Differ.* **40**, 181-215.
Wilton, S. D. and Fletcher, S. (2006). Modification of pre-mRNA processing: application to dystrophin expression. *Curr. Opin. Mol. Ther.* **8**, 130-135.
Zhang, Y., Chen, H. S., Khanna, V. K., de Leon, S., Phillips, M. S., Schappert, K., Britt, B. A., Brownell, A. K. W. and MacLennan, D. H. (1993). A mutation in the human ryanodine receptor gene associated with central core disease. *Nat. Genet.* **5**, 46-50.
Zhou, W., Saint-Amant, L., Hirata, H., Cui, W. W., Sprague, S. M. and Kuwada, J. Y. (200**6**). Non-sense mutations in the dihydropyridine receptor β1 gene, *CACNB1*, paralyze zebrafish *relaxed* mutants. *Cell Calcium* **39**, 227-236.